

Model Based Training, Detection and Pose Estimation of Texture-Less 3D Objects in Heavily Cluttered Scenes

Stefan Hinterstoisser¹, Vincent Lepetit³, Slobodan Ilic¹, Stefan Holzer¹, Gary Bradski², Kurt Konolige², Nassir Navab¹

¹CAMP, Technische Universität München (TUM), Germany

²Industrial Perception, Palo Alto, CA, USA

³CV-Lab, École Polytechnique Fédérale de Lausanne (EPFL), Switzerland

Abstract. We propose a framework for automatic modeling, detection, and tracking of 3D objects with a Kinect. The detection part is mainly based on the recent template-based LINEMOD approach [1] for object detection. We show how to build the templates automatically from 3D models, and how to estimate the 6 degrees-of-freedom pose accurately and in real-time. The pose estimation and the color information allow us to check the detection hypotheses and improves the correct detection rate by 13% with respect to the original LINEMOD. These many improvements make our framework suitable for object manipulation in Robotics applications. Moreover we propose a new dataset made of 15 registered, 1100+ frame video sequences of 15 various objects for the evaluation of future competing methods.



Fig. 1. 15 different texture-less 3D objects are simultaneously detected with our approach under different poses on heavy cluttered background with partial occlusion. Each detected object is augmented with its 3D model. We also show the corresponding coordinate systems.

1 Introduction

Many current vision applications, such as pedestrian tracking, dense SLAM [2], or object detection [1], can be made more robust through the addition of depth information. In this work, we focus on object detection for Robotics and Machine Vision, where it is important to efficiently and robustly detect objects and

estimate their 3D poses, for manipulation or inspection tasks. Our approach is based on LINEMOD [1], an efficient method that exploits both depth and color images to capture the appearance and 3D shape of the object in a set of templates covering different views of an object. Because the viewpoint of each template is known, it provides a coarse estimate of the pose of the object when it is detected.

However, the initial version of LINEMOD [1] has some disadvantages. First, templates are learned online, which is difficult to control and results in spotty coverage of viewpoints. Second, the pose output by LINEMOD is only approximately correct, since a template covers a range of views around its viewpoint. And finally, the performance of LINEMOD, while extremely good, still suffers from the presence of false positives.

In this paper, we show how to overcome these disadvantages, and create a system based on LINEMOD for the automatic modeling, detection, and tracking of 3D objects with RGBD sensors. Our main insight is that a 3D model of the object can be exploited to remedy these deficiencies. Note that accurate 3D models can now be created very quickly [2–5], and requiring a 3D model beforehand is not a disadvantage anymore. For industrial applications, a detailed 3D model often exists before the real object is even created.

Given a 3D model of an object, we show how to generate templates that cover a full view hemisphere by regularly sampling viewpoints of the 3D model. We also show how the 3D model can be used to obtain a fine estimate of the object pose, starting from the one provided by the templates. Together with a simple test based on color, this allows us to remove false positives, by checking if the object under the recovered pose aligns well with the depth map. Moreover, we show how to define the templates only with the most useful appearance and depth information, which allows us to speed up the template detection stage. The end result is a system that significantly improves the original LINEMOD implementation in performance, while providing accurate pose for applications.

In short, we propose a framework that is easy to deploy, reliable, and fast enough to run in real-time. We also provide a dataset made of 15 registered, 1100+ frame video sequences of 15 various objects for the evaluation of future competing methods. In the remainder of this paper we first discuss related work, briefly describe the approach of LINEMOD, introduce our method, represent our dataset and present an exhaustive evaluation.

2 Related Work

3D object detection and localization is a difficult but important problem with a long research history. Methods have been developed for detection in photometric images and range images, and more recently, in registered color/depth images. We discuss these below.

Camera Images. We can divide image-based object detection into two broad categories: learning-based and template approaches. Learning-based systems generalize well to the objects of particular class like human faces [6], cars [7, 8], or

other objects [9]. Their main limitations are the limited set of object poses they accept, and the large training database and time. In general, they also do not return an accurate estimate of the object 3D pose.

To overcome these limitations, researchers tried to learn the object appearance from 3D models [7, 8, 10]. The approach of Stark *et al.* [7] relies only on 3D CAD models of cars and Liebelt and Schmid [8] combine geometric shape and pose priors with natural images. Both of these approaches work well and also generalize to object classes, but they are not real-time capable, require expensive training and cannot handle clutter and occlusions well. In [10] authors use a number of viewpoint-specific shape representations to model the object category. They rely on contours and introduce a novel feature called BOB (bag of boundaries), which at a given point in the image is a histogram of boundaries from image contours in training images. This feature is later used in the shape context descriptor for template matching. While it generalizes well, it is far from real-time and cannot find a precise 3D pose. In contrast, our method is real-time capable, can learn new objects online from 3D models, can handle large amount of clutter and moderate occlusions and can detect multiple objects simultaneously.

As discussed in [1], template-based approaches [11–14] typically do not require large training sets or time, as the templates are acquired quickly from views of the object. However, all these approaches are either susceptible to background clutter or too slow for real-time performance.

Range Images. Detection of 3D objects in range data has a long history; a review can be found in [15]. One of the standard approaches for object pose estimation is ICP [16]; however this approach requires an initial estimate and is not suited for object detection. Approaches based on 3D features are more suitable and are usually followed by ICP for the pose refinement. Some of these methods (which assume that a full 3D model is available) include spin-images [17], point pairs [18, 19], and point-pair histograms [20, 21]. These methods are usually computationally expensive, and have difficulty in scenes with clutter. The method of Drost *et. al* [18] can deal with clutter; however, its efficiency and performance depend directly on the complexity of the 3D scene, which makes it difficult to use in real-time applications.

RGBD Images. In recent years, a number of methods that rely on RGBD sensors have been introduced—among them [22] which is subject to object classification, pose estimation and reconstruction. Similar to us the training data set is composed of depth and image intensity cues and the object classes are detected using a modified Hough transform. While being quite effective in real applications these approaches still require exhaustive training on large data sets. In [23] Lei *et al.* study the recognition problem at both the category and the instance level. In addition they provide a large data set of 3D objects. However, they have neither demonstrated that their approach work on heavily cluttered scenes in real time nor that it returns 3D pose as our method does.

3 Approach

Our approach to object detection is based on LINEMOD [1]. LINEMOD is an efficient method to detect multi-modal templates in the Kinect output, a depth map registered to a color image. The LINEMOD templates sample the possible appearances of the objects to detect, and are built from densely sampled image gradients and depth map normals. When a template is found, it provides not only the object’s 2D location in the image, but also a coarse estimate of its pose, as the templates can easily be labeled with this information.

In the remainder of the paper, we will show how we generate the templates automatically from a 3D model with a regular sampling. We also show how we speed up detection time by keeping only the most useful information in the templates, how we compute a fine estimate of the object 3D pose, and how we exploit this pose and the object color to detect outliers.

3.1 Exploiting a 3D Model to Create the Templates

In contrast to online learning approaches [1, 14, 24–26], we build a set of templates automatically from CAD 3D models. This has several advantages. First, online learning requires physical interaction of a human operator or a robot with their environment, and therefore takes time and effort. Furthermore, it usually takes an educated user and careful manual interaction to collect a well sampled training set of the object that covers the whole pose range. Online methods usually follow a greedy approach and they are not guaranteed to lead to optimal results in terms of trade-off between efficiency and robustness.

3.1.1 Viewpoint Sampling: Viewpoint sampling is crucial in LINEMOD. We have to balance the trade-off between the coverage of the object for reliability and the number of template for efficiency. As in [27], we solve this problem by recursively dividing an icosahedron, the largest convex regular polyhedron. We substitute each triangle into four almost equilateral triangles, and iterate several times. As illustrated in Fig. 2, the vertices of the resulting polyhedron give us then the two out-of-plane rotation angles for the sampled pose with respect to the coordinate center. In practice we stop at 162 vertices on the upper hemisphere for a good trade-off. Two adjacent vertices are then approximately 15 degrees apart. In addition to the these two out of plane rotations, we also created templates for different in-plane rotations. Furthermore, we generate templates at different scales by using different sized polyhedrons, using a step size of 10 cm.

3.1.2 Reducing Feature Redundancy: LINEMOD relies on two different features: color gradients, computed from the color image, and surface normals, computed from the object 3D model. Both are discretized to a few values by the algorithm. The color gradients are taken at each image location as the gradient of largest magnitude over the 3 color channels. The LINEMOD templates are made from these two features computed densely. We show here that we can

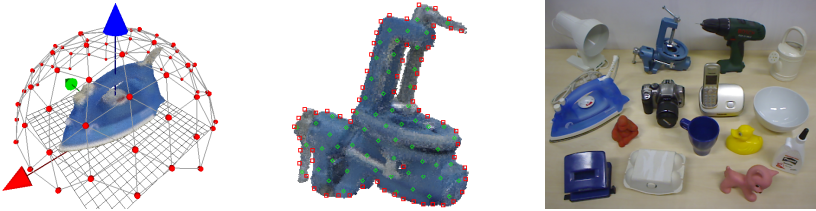


Fig. 2. **Left:** Sampling the viewpoints of the upper hemisphere for template generation: Red vertices represent the virtual camera centers used to generate templates. Note, that the camera centers are uniformly sampled. **Middle:** The selected features: Color gradient features are displayed in red, surface normal features in green. The features are quasi uniformly spread over the areas where they represent the object best. **Right:** 15 different texture-less 3D objects used in our experiments.

consider only a subset of the features used in LINEMOD. This speeds up the detection with no loss of accuracy.

Color Gradient Features: We keep only the main color gradient features located on the contour of the object silhouette, because we focus on texture-less objects which exhibit no or only little texture on the interior of the object silhouette, and because the texture of a given CAD 3D model is not always available.

For each sampled pose generated by the method described above, we first compute the object silhouette by projecting the 3D model under this pose. By subtracting the eroded silhouette from its original version we quickly obtain the silhouette contour. We then compute all the color gradients that lie on the silhouette contour and sort them with respect to their magnitudes. This is important since our silhouette edge is not guaranteed to be only one pixel broad. We then use a greedy approach where we iterate through this sorted list, starting from the gradient with the strongest magnitude, and take the first feature that appears in this list. We then remove from the list the features whose image locations are close—according to some distance threshold—to the picked feature location, and we iterate.

If we have finished iterating through the list of features before a desired number of features is selected, we decrease the distance threshold by one and start the process again. The threshold is initially set to the ratio of the area covered by the silhouette and the number of features that are supposed to be selected. This heuristic is reasonable since the silhouette contour is usually a one pixel broad edge such that the initial threshold is simply the maximal possible distance between two features if these are spread uniformly on an ideal one pixel broad silhouette. As a result, our efficient method ensures that the selected features are both robust and, at the same time, almost uniformly spread on the silhouette (see Fig. 2).

Surface Normal Features: In contrast to color gradient features, we chose the surface normal features to be selected on the interior of the object silhouette.

This is because the surface normals on the borders of the projected object are often not estimated reliably, or not recovered at all.

As in LINEMOD we discretize the normals computed from the depth map by considering their orientations. The first difference is that in the case of the template generation, the depth map is computed from the object 3D model, not acquired by the Kinect.

We first remark that normals surrounded by normals of similar orientation are recovered more reliably. We therefore want to keep these normals during the creation of the template, and discard the less stable ones. To do so, we first create a mask for each of the 8 possible values of discretized orientations from the depth map generated for the object under the considered pose.

For each of the 8 masks, we then weight each normal with the distance to the mask boundary. Large distances indicate normals surrounded with normals of similar orientation. Small distances indicate normals surrounded by different normals, or normals close to the object silhouette boundaries, and we first directly reject the normals with a weight smaller than a specific distance—we use 2 in practice.

However, we can not rely on the weights only to select the normals we want to keep among the remaining ones. This is because large areas with similar normals would have a too great influence on the resulting template, and therefore, we normalize the weights by the size of the mask they belong to.

We then proceed as for the selection of the color gradients. We first create a list of the surface normals, ranked according to their normalized weights, and iteratively select the normals we keep in the final template. It ensures an quasi uniform spreading of the selected normals (see Fig. 2). Here, the threshold is set to the square root of the ratio of the area covered by the rendered object and the number of features we want to keep.

3.2 Postprocessing Detections

For each template detected by LINEMOD—starting with the one with the highest similarity score, we first check the consistency of this detection by comparing the object color with the content of the color image at its location. If it passes the test, we estimate the 3D pose of the corresponding object. We reject all detections whose 3D pose estimates have not converged properly. Taking the first n detections that passed all checks, we do a final pose estimate for the best of them. We use this final estimate in an ultimate depth test for the validity of the detection. As shown in the results section, these additional tests make our approach much more reliable than LINEMOD.

3.2.1 Coarse Outlier Removal by Color: Each detected template provides a coarse estimate of the object pose that is good enough for an efficient check based on color information. We consider the pixels that lie on the object projection according to the pose estimate, and count how many of them have the expected color. We decide a pixel has the expected color if the difference between its hue

and the object hue (modulo 2π) is smaller than a threshold—considering the hue makes the test robust to light changes. If the percentage of pixels that have their expected color is not large enough (at least 70% in our implementation), we reject the detection as false positive.

In practice we do not take into account the pixels that are too close to the object projection boundaries, to be tolerant to the inaccuracy of the current pose estimate. This can be done efficiently by eroding the object projection beforehand.

We still have to handle black and white objects. Since black and white are not covered by the hue component, we map them to the hue values of similar colors: black to blue and white to yellow. This is done by checking the corresponding saturation and value component before we compute the absolute difference. In case the value component is below a threshold t_v , we set the hue value to blue. If the value component is larger than t_v and the saturation component below a threshold t_s , we set the hue component to yellow. In our case $t_s = t_v = 0.12$.

3.2.2 Fast Pose Estimation and Outlier Rejection based on Depth: For the detections that passed the previous color check, we refine the pose estimate provided by the template detection. This is performed with the Iterative Closest Point algorithm to align the 3D model surface with the depth map. The initial translation is estimated from the depth values covered by the initial model projection.

For efficiency, we first subsample the 3D points from the depth map that lie on the object projection or close to it. To speed up point-to-point matching, we use the efficient voxel-based ICP method of [28], which relies on a grid that can be pre-computed for each object. For robustness, at each iteration i , we compute the alignment using only the inlier 3D points. The inlier points are the ones that fall within a distance to the 3D model smaller than an adaptive threshold t_i . t_0 is initialized to the size of the object, t_{i+1} is set to three times the average distance of the inliers to the 3D model at time i . After convergence, if the average distance of the inliers to the 3D model is too large, we reject the detection as false positive.

We repeat this until $n = 3$ detections passed this check or no detections are left. Then we perform a slower but finer ICP for the best of these n detections by considering all the points from the depth map that lie on the object projection or close to it. The best detection is found by comparing the number of inliers and their average distance to the 3D model. The final ICP is followed by a final depth test. For that, we consider the pixels that lie on the object projection according to the final pose estimate, and count how many of them have the expected depth. We decide a pixel has the expected depth if the difference between its depth value and the projected object depth is smaller than a threshold. If the percentage of pixels that have their expected depth is not large enough (at least 70% in our implementation), we finally reject the detection as false positive. Otherwise, we say that the object was found with the final pose.



Fig. 3. 15 different texture-less 3D objects are simultaneously detected under different poses on heavy cluttered background with partial occlusion and illumination changes. Each detected object is augmented with its 3D model and its coordinate systems.

4 Experiments

For comparison, we created a large dataset of 15 registered video sequences of 15 texture-less 3D objects. Each object was stucked to the center of a planar board with markers attached to it, for model and image acquisition. The markers on the board provided the corresponding ground truth poses. Each object was reconstructed first using a set of images and the corresponding poses using a simple voxel based approach. After reconstruction, we added close range and far range 2D and 3D clutter to the scene and took the evaluation sequences. Each sequence contains more than 1,100 real images from different view points. In order to guarantee a well distributed pose space sampling of the dataset pictures, we uniformly divided the upper hemisphere of the objects into equally distant pieces and took at most one image per piece. As a result, our sequences provide uniformly distributed views from 0-360 degree around the object, 0-90 degree tilt rotation, 65 cm-115 cm scaling and ± 45 degree in-plane rotation. For each object, we visualized the cameras color coded with respect to their distance to the object center in the second column of Figs. 5 and 6.

Since it was already shown in [29] that LINEMOD outperforms DOT [14], HOG [30], TLD [26] and the method of Steger *et al.* [13], we compare our method only to the one of Drost *et al.* [18]. For [18], we use the binaries kindly provided by the authors that run on Intel Xeon E5345 processor with 2.33 GHz and 32 GB RAM. All the other experiments were performed on a standard notebook with an Intel i7-2820QM processor with 2.3 GHz and 8 GB of RAM. For obtaining the image and the depth data we used the Primesense^(tm) PSDK 5.0 device.

4.1 Robustness

In order to evaluate our approach, we first have to define an appropriate matching score for a 3D model \mathcal{M} : having the ground truth rotation \mathbf{R} and translation

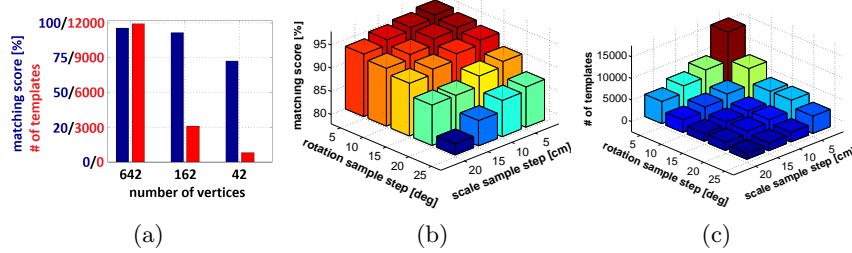


Fig. 4. Quality of the detections for drilling machine data set with respect to the viewpoint sampling steps. (a) The matching scores for different numbers of vertices (see Sec. 3.1). A good trade-off between speed and robustness are 162 vertices for the upper hemisphere. (b),(c): the matching score decreases if the sample steps increase. We also display the number of templates with respect to the sampling steps: we made sure that all necessary poses were covered. A good trade-off between speed and robustness is a rotation sampling step of 15 degree and a scale sampling step of 10 cm.

Approach	Our Appr.	Drost[18]	LINEMOD3	LINEMOD1	Our Appr.	Drost[18]
Sequence (#pics)	Matching Score				Speed	
Ape (1235)	95.8%	86.5%	86.3%	69.4%	127ms	22.7s
Bench Vise (1214)	98.7%	70.7%	98.0%	94.0%	115ms	2.94s
Driller (1187)	93.6%	87.3%	91.8%	81.3%	121ms	2.65s
Cam (1200)	97.5%	78.6%	93.4%	79.5%	148ms	2.81s
Can (1195)	95.4%	80.2%	91.3%	79.5%	122ms	1.60s
Iron (1151)	97.5%	84.9%	95.9%	88.8%	116ms	3.18s
Lamp (1226)	97.7%	93.3%	97.5%	89.8%	125ms	2.29s
Phone (1224)	93.3%	80.7%	88.3%	77.8%	157ms	4.70s
Cat (1178)	99.3%	85.4%	97.9%	88.2%	111ms	7.52s
Hole punch (1236)	95.9%	77.4%	90.5%	78.4%	110ms	8.30s
Duck (1253)	95.9%	46.0%	91.4%	75.9%	104ms	6.97s
Cup (1239)	97.1%	68.4%	87.9%	80.7%	105ms	16.7s
Bowl (1232)	99.9%	95.7%	99.7%	99.5%	97ms	5.18s
Box (1252)	99.8%	97.0%	99.8%	99.1%	101ms	2.94s
Glue (1219)	91.8%	57.2%	80.9%	64.3%	135ms	4.03s
Average (18241)	96.6%	79.3%	92.7%	83.0%	119ms	6.3s

Table 1. Recognition rates for $k_m = 0.1$. The first column gives the results of our method using automatically generated templates (see Sec. 3.1). The second and third columns give recognition numbers if no postprocessing is performed. For the second column, we use the best (with respect to the ground truth) out of the first $n = 3$ detections with the highest similarity score. For the third column, we only evaluate the detection with the highest similarity score. In the fourth and fifth column, we give the average runtime of our method and the one of Drost *et al.* [18] per frame.

T and the estimated rotation $\tilde{\mathbf{R}}$ and translation $\tilde{\mathbf{T}}$, we compute the average distance of all model points \mathbf{x} from their transformed versions:

$$m = \operatorname{avg}_{\mathbf{x} \in \mathcal{M}} \|(\mathbf{Rx} + \mathbf{T}) - (\tilde{\mathbf{R}}\mathbf{x} + \tilde{\mathbf{T}})\|. \quad (1)$$

We say that the model was correctly detected and the pose correctly estimated if $k_m d \geq m$ where k_m is a chosen coefficient and d is the diameter of \mathcal{M} . We still have to define a matching score measure for objects that are ambiguous or have a subset of views under which they appear to be ambiguous. Such objects ("cup", "bowl", "box" and "glue") are shown in Fig. 6. We define the corresponding matching score as:

$$m = \text{avg}_{\mathbf{x}_1 \in \mathcal{M}} \min_{\mathbf{x}_2 \in \mathcal{M}} \|(\mathbf{R}\mathbf{x}_1 + \mathbf{T}) - (\tilde{\mathbf{R}}\mathbf{x}_2 + \tilde{\mathbf{T}})\|. \quad (2)$$

Since it was already shown in [29] that LINEMOD outperforms DOT [14], HOG [30], TLD [26] and the method of Steger *et al.* [13], we evaluate our new pipeline with the approach of Drost *et al.* [18]. This approach – contrary to the before mentioned ones – does not only perform detection but also pose estimation of general 3D objects. For our experiments, we set $n = 3$ and used the optimal training parameters as described in Sec. 4.3. As one can see in the graphs shown in Fig. 5 and 6, our new approach outperforms Drost *et al.* [18].

In addition, we compared the output of our new pipeline to the detection results of LINEMOD. For the latter, we simply used the pose composed by the rotation under which the detected template was created and the translation coming from the depth map. Here, we evaluated two strategies: for the first one, we only took the pose of the detected template whose similarity score was largest (LINEMOD1). Since our new pipeline evaluates several hypotheses, we also added curves where we took the best pose with respect to the ground truth one out of the three best detected templates (LINEMOD3). For both cases, we can see that our new pipeline drastically increases the recognition performance.

We also show the matching results for $k_m = 0.1$ in Table 1. Matches with $k_m = 0.1$ are also found visually correct. In this table, we see that our new pipeline outperforms the approach of Drost *et al.* [18] by average 17.3% and improves the recognition results by average 13% w.r.t. the original LINEMOD.

Furthermore, we also evaluated our new approach on the ape, duck and cup dataset of [1] where we compared our automatically trained LINEMOD against the manually learned LINEMOD. Our new pipeline obtains almost no false positives and a superior true positive rate of 98.7% for the cup sequence (compared to [1]: 96.8%), 98.2% for the ape sequence (compared to [1]: 97.9%) and 99.5% for the duck sequence (compared to [1]: 97.9).

4.2 Speed

As we see in Tab. 1, our whole recognition pipeline needs in average 119ms to detect an object in the pose range of 0-360 degree around the object, 0-90 degree tilt rotation, 65 cm-115 cm scaling and ± 45 degree in-plane rotation. This is 53 times faster than the approach of Drost *et al.* and allows real-time recognition. To cover this pose range we need 3,115 templates. Unoptimized training lasts from 17 seconds for the "ape" object to 50 seconds for the "bench vise" object and is dependent on the number of vertices to render.

4.3 Choosing Training Sample Parameters

In order to choose the right parameters for training, we initially took the drill sequence and evaluated our method with respect to the training parameters. As we can see in the first graph of Fig. 4, sampling the viewpoints with 162 vertices is a good trade-off between robustness and the number of templates which have to be matched. The speed performance of our approach is proportional to this number and thus, using less templates implies shorter runtime. In addition we made experiments, how the sampling of the scale and the in-plane rotation influences the robustness and the runtime. As we can see in middle and right graphs of Fig. 4, a good trade-off is a scale step of 10 cm and a rotation step of 15 degrees. As we found out, the choice of these parameters gave very good results for all objects in our database. Therefore, we set them once and for all.

5 Conclusion

We have presented a framework for automatic learning, detection and pose estimation of 3D objects using a Kinect. As a first contribution, we showed how we automatically reduce feature redundancy for color gradients and surface normals and how we automatically learn templates from a 3D model. For the latter, we provide a solution of pose space sampling which guarantees a good trade-off between detection speed and robustness. As a second contribution, we provided novel means for efficient postprocessing and showed that the pose estimation and the color information allow us to check the detection hypotheses and to improve the correct detection rate by 13% with respect to the original LINEMOD. Furthermore, we showed that we significantly outperform the approach of Drost *et al.* [18]—a commercial state-of-the-art detection approach that is able to estimate the object pose. Our final contribution is the proposal of a new dataset made of 15 registered, 1100+ frame video sequences of 15 various texture-less objects for the evaluation of future competing methods. The novelty of our sequences with respect to state-of-the-art datasets is the combination of the following features: First, for each sequence and each image, we provide the corresponding 3D model of the object and its ground truth poses. Second, each sequence uniformly covers the complete pose space around the registered object. Third, each image contains heavy close range and far range 2D and 3D clutter.

References

1. Hinterstoisser, S., Cagniart, C., Holzer, S., Ilic, S., Konolige, K., Navab, N., Lepetit, V.: Multimodal Templates for Real-Time Detection of Texture-Less Objects in Heavily Cluttered Scenes. In: ICCV. (2011)
2. Newcombe, R.A., Izadi, S., Hilliges, O., Molyneaux, D., Kim, D., Davison, A.J., Kohli, P., Shotton, J., Hodges, S., Fitzgibbon, A.: KinectFusion: Real-Time Dense Surface Mapping and Tracking. In: ISMAR. (2011)
3. Pan, Q., Reitmayr, G., Drummond, T.: ProFORMA: Probabilistic Feature-based On-line Rapid Model Acquisition. In: BMVC. (2009)
4. Weise, T., Wismer, T., Leibe, B., Gool, L.V.: In-hand Scanning with Online Loop Closure. In: International Workshop on 3-D Digital Imaging and Modeling. (2009)

5. Newcombe, R.A., Lovegrove, S.J., Davison, A.J.: DTAM: Dense Tracking and Mapping in Real-Time. In: ICCV. (2011)
6. Viola, P., Jones, M.: Fast Multi-View Face Detection. In: CVPR. (2003)
7. Stark, M., Goesele, M., Schiele, B.: Back to the Future: Learning Shape Models from 3D Cad Data. In: BMVC. (2010)
8. Liebelt, J., Schmid, C.: Multi-View Object Class Detection With a 3D Geometric Model. In: CVPR. (2010)
9. Ferrari, V., Jurie, F., Schmid, C.: From Images to Shape Models for Object Detection. IJCV (2009)
10. Payet, N., Todorovic, S.: From contours to 3d object detection and pose estimation. In: ICCV. (2011) 983–990
11. Gavrila, D., Philomin, V.: Real-Time Object Detection for “smart” Vehicles. In: ICCV. (1999)
12. Huttenlocher, D., Klanderman, G., Rucklidge, W.: Comparing Images Using the Hausdorff Distance. TPAMI (1993)
13. Steger, C.: Occlusion Clutter, and Illumination Invariant Object Recognition. In: International Archives of Photogrammetry and Remote Sensing. (2002)
14. Hinterstoisser, S., Lepetit, V., Ilic, S., Fua, P., Navab, N.: Dominant Orientation Templates for Real-Time Detection of Texture-Less Objects. In: CVPR. (2010)
15. Mian, A.S., Bennamoun, M., Owens, R.A.: Automatic Correspondence for 3D Modeling: an Extensive Review. International Journal of Shape Modeling (2005)
16. Zhang, Z.: Iterative Point Matching for Registration of Free-Form Curves. IJCV (1994)
17. Johnson, A.E., Hebert, M.: Using Spin Images for Efficient Object Recognition in Cluttered 3 D Scenes. TPAMI (1999)
18. Drost, B., Ulrich, M., Navab, N., Ilic, S.: Model Globally, Match Locally: Efficient and Robust 3D Object Recognition. In: CVPR. (2010)
19. Mian, A.S., Bennamoun, M., Owens, R.: Three-Dimensional Model-Based Object Recognition and Segmentation in Cluttered Scenes. TPAMI (2006)
20. Rusu, R.B., Blodow, N., Beetz, M.: Fast Point Feature Histograms (FPFH) for 3D Registration. In: International Conference on Robotics and Automation. (2009)
21. Tombari, F., Salti, S., Stefano, L.D.: Unique Signatures of Histograms for Local Surface Description. In: ECCV. (2010)
22. Sun, M., Bradski, G.R., Xu, B.X., Savarese, S.: Depth-Encoded Hough Voting for Joint Object Detection and Shape Recovery. In: ECCV. (2010)
23. Lai, K., Bo, L., Ren, X., Fox, D.: Sparse distance learning for object recognition combining rgb and depth information. In: ICRA. (2011) 4007–4013
24. Grabner, M., Grabner., H., Bischof, H.: Learning Features for Tracking. In: CVPR. (2007)
25. Ozysal, M., Calonder, M., Lepetit, V., Fua, P.: Fast Keypoint Online Learning and Recognition. TPAMI (2010)
26. Kalal, Z., Matas, J., Mikolajczyk, K.: P-N Learning: Bootstrapping Binary Classifiers by Structural Constraints. In: CVPR. (2010)
27. Hinterstoisser, S., Benhimane, S., Lepetit, V., Fua, P., Navab, N.: Simultaneous Recognition and Homography Extraction of Local Patches With a Simple Linear Classifier. In: BMVC. (2008)
28. Fitzgibbon, A.: Robust Registration fo 2D and 3D Point Sets. In: BMVC. (2001)
29. Hinterstoisser, S., Ilic, S., Sturm, P., Navab, N., Fua, P., Lepetit, V.: Gradient Response Maps for Real-Time Detection of Texture-Less Objects. TPAMI (2012)
30. Dalal, N., Triggs, B.: Histograms of Oriented Gradients for Human Detection. In: CVPR. (2005)

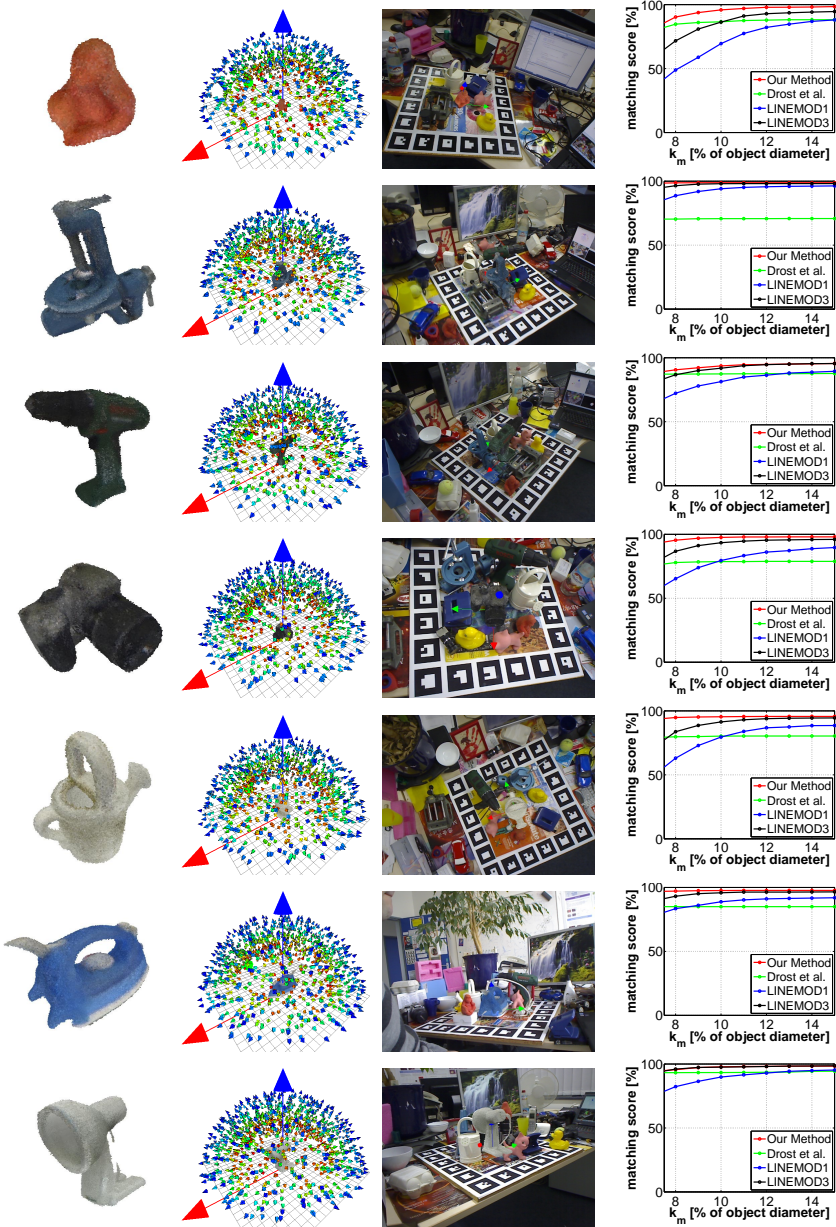


Fig. 5. In our experiments, different texture-less 3D objects are detected in real-time under different poses on heavy cluttered background. **Left:** Some 3D reconstructed models. **Middle Left:** The pose space of the dataset images. The distance of the cameras to the object is color coded. **Middle Right:** One test image with the correctly recognized object. The 3D model of the object is augmented. **Right:** The matching scores with respect to different k_m . **The datasets is public available at <http://campar.in.tum.de/twiki/pub/Main/StefanHinterstoesser>.**

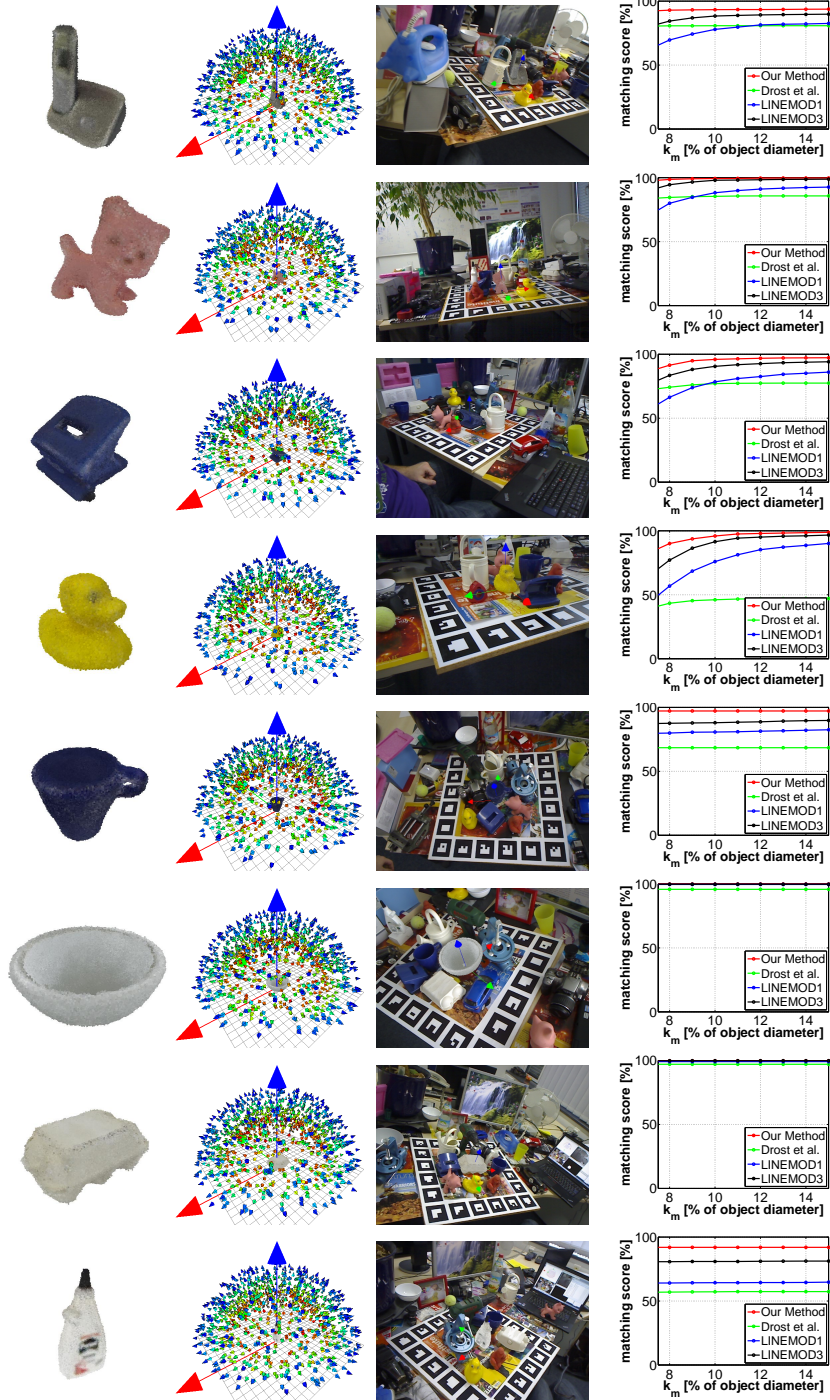


Fig. 6. Another set of 3D objects we used in our extensive experiments. The datasets is public available at <http://campar.in.tum.de/twiki/pub/Main/StefanHinterstoesser>.